CrystEngComm

Accepted Manuscript

ROYAL SOCIETY OF CHEMISTRY

www.rsc.org/crystengcomm

TOC

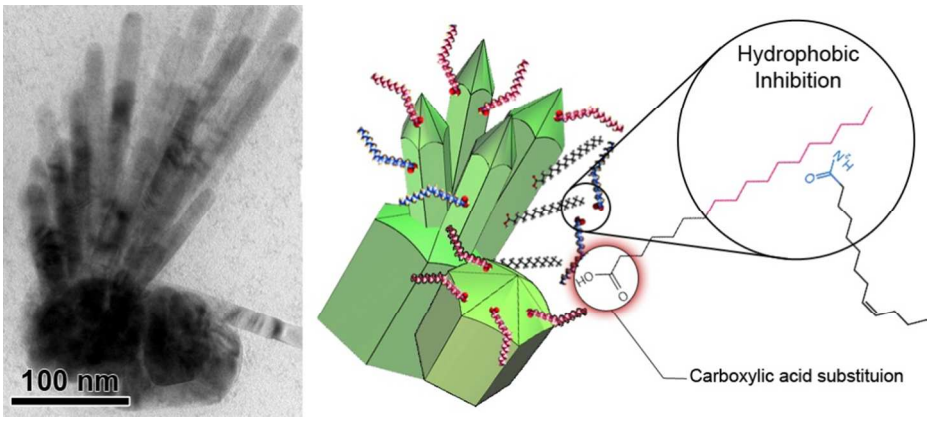

Crystal growth and self-assembly in iono-covalent nanomaterials can be directed via lipophilic interactions between a variety of metal soaps and amphiphilic lipids.

Cite this: DOI: 10.1039/c0xx00000x

www.rsc.org/xxxxxx

ARTICLE

Self-assembly and secondary nucleation in ZnO nanostructures derived from a lipophilic precursor

Wee Siong Chiu,*[a] Alireza Yaghoubi,*[b] Mei Yuen Chia,[a] Noor Hamizah Khanis,[a] Saadah A. Rahman,[a] Poi Sim Khiew,[c] and Yu-Lun Chueh[d]

Received (in XXX, XXX) Xth XXXXXXXXX 20XX, Accepted Xth XXXXXXXXX 20XX
DOI: 10.1039/b000000x

The influence of organically capped nucleation on morphogenesis of zinc oxide (ZnO) as a technologically important iono-covalent material has been extensively investigated. However, the effect of lipid-lipid interactions on selective adsorption and mechanism of growth is largely unknown. Here, we demonstrate a novel route toward synthesis of various ZnO nanostructures using zinc stearate, a metal soap, rather than the commonly utilised polar-soluble salts. Study of a variety of amphiphilic ligands suggests that during decomposition, secondary carboxylic acids substitute for primary aliphatic tails in the precursor. In this regard, saturated and unsaturated fatty acids appear to influence the rate of progression quite differently. On the other hand, in the early stages of growth, amine adsorbates are inhibited by lipophilic tails of carboxylic acids, leading to a multi-step growth. The subsequent self-assembly of these nanorods into bundles is accompanied by recrystallisation of their stems and formation of planar defects which promote random secondary nucleation.

Introduction

Interaction of organic supramolecular systems like collagens with inorganic building blocks is central to the self-assembly of hard tissues through biomineralisation.[1] Inspired by the highly ordered arrangement of such biogenic minerals, scientists in recent years have intensively pursued the possibility of replicating a similar process to exert control over the formation of inorganic nanostructures.[2] Amphiphilic lipids, especially fatty acids, owing to their low cost and ease of access, have been among the most popular capping agents for controlled synthesis of nanoparticles either as extracted from an organometallic compound[3] or as combined with other precursors.[4] However, majority of relevant reports are essentially optimised recipes which lead to only certain families of materials by shape or chemistry. As a result, selective behaviour of each organic compound with respect to nucleation and growth in solution phase synthesis is still under scrutiny.[5]

Wurtzite ZnO (space group $P6_3mc$) not only because of its wide range of potential applications in optoelectronic,[6,7] piezoelectric[8] and sensing devices,[9,10] but more importantly, as a platform with strong electric dipole moment due to its noncentrosymmetry[11] is a good candidate for further understanding the effect of polarisability on formation of nanomaterials. Nicholas and colleagues have recently examined the selective adsorption of carboxylic acids and amines to the polar and non-polar facets of ZnO, respectively.[12] Their systematic study finally confirmed the earlier reports that addition of ligands during hydrolysis of zinc salts could prevent growth in certain directions.[13,14]

Common precursors for synthesis of ZnO through solvothermal synthesis often include sources of zinc ions in form of extremely polar solutes, for example zinc nitrate,[15,16] zinc chloride[17] and zinc acetate, either as dihydrate[18] or anhydrous.[19,20] Non-polar precursors, on the other hand, have been less extensively explored. Zinc oleate for example as a non-polar fatty acid salt was used to synthesise triangular nanocrystals[21] as well as long nanowires.[22] In the latter, the high aspect ratio was associated with the selective adsorption of oleate ions, although the effect of alkaline cations on morphogenesis was clearly dominant and no indication of possible lipid-mediated growth was found.

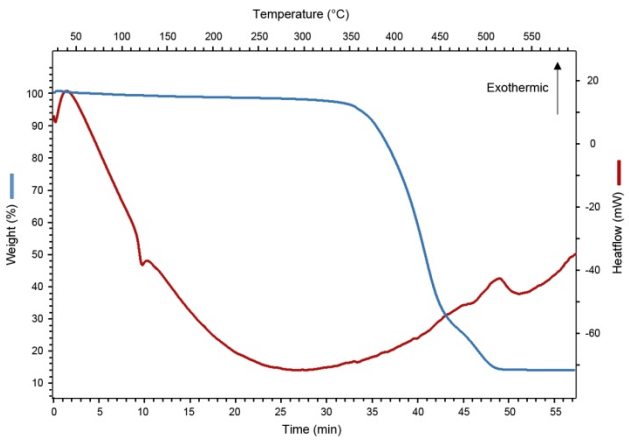

Fig. 1. TGA/DSC curves for zinc stearate reveals a relative thermal equilibrium with negligible variation in heat flow between 250°C and 350°C. The reaction up to this interval is largely endothermic.

In this study, we establish a new approach for synthesis of ZnO nanostructures in solution phase by non-hydrous pyrolysis of zinc stearate which its surface chemistry is very similar to that of a saturated lipid. Investigating the interactions of various capping agents with the lipophilic precursor under a system with constant heat flow is expected to reveal the underlying process of organic decomposition prior to nucleation and its influence on the kinetics of growth. This is especially of interest considering that in nature, complex supramolecules which serve as templates for further organisation of inorganic tectons,[23] are often a byproduct of interactions between organic functional groups. Naturally occurring vesicles in cells and their artificially created counterparts (liposomes) for example, are essentially assemblies of lipidic membranes which later can be used to create hierarchically integrated hybrids with inorganic nanoparticles.[24] Therefore, the possibility to control microscopic structures solely through the preliminary polar/ non-polar interactions of simple organic molecules may ultimately enable the development of a universal technique for bottom-up fabrication of devices from a large varieties of lipophilic metal soaps and amphiphilic lipids.

Methodology

Synthesis of ZnO nanostructures

In a typical synthesis, 3.3 mmol of zinc stearate ($Zn(C_{18}H_{35}O_2)_2$, Meryer Chemicals) with 1.5 mmol of various capping agents, namely oleic acid ($C_{18}H_{34}O_2$, Sigma-Aldrich, 99%), stearic acid ($CH_3(CH_2)_{16}COOH$, Sigma-Aldrich, reagent grade 95%), palmitic acid ($CH_3(CH_2)_{14}COOH$, Sigma-Aldrich, 99%) and oleylamine ($C_{18}H_{37}N$,Sigma-Aldrich, technical grade 70%) or a combination thereof was loaded into a 250 mL four neck flask equipped with an Allihn condenser. The mixture along with 50 mL of 1-octadecene ($C_{18}H_{36}$, Sigma-Aldrich, technical grade 90%) as solvent was heated to 120^{o}C using a heating mantle (Glas-Col). The temperature was regulated by a JKEM Reaction Controller (SYR-DTC) under vigorous stirring. A vacuum pump was used to degas the reaction environment and backfill it with argon to remove any residual amount of water and oxygen. After several rounds of degassing, the temperature was ramped to 317^{o}C at a constant rate after which the mixture was refluxed for 6 hours. Formation of ZnO nanostructures was subsequently indicated by a temporal change in the physical appearance of the mixture. In particular, the initially clear solution turned into turbid precipitates with a distinctive pale greenish or yellowish colour depending on the ligands used.

Upon annealing for another 6 hours, the reaction was terminated by removing the flask from the heating mantle and cooling down the mixture to room temperature under the flow of argon. The as-synthesised products were dispersed in hexane and precipitated by acetone after which the precipitate was centrifuged at 4000 rpm for 20 minutes to retrieve the ZnO nanostructures. This process was repeated at least three times to remove any unreacted precursors as well as excessive capping ligands. Finally, the samples were dispersed in hexane to form stable suspensions.

Characterisations

The morphology as well as the kinetics of growth for ZnO nanostructures were characterised on a JEOL JEM-2100F high-resolution transmission electron microscope (HRTEM) at an operating voltage of 200 kV. Samples were prepared by drop-casting the hexane dispersion on a 300 mesh amorphous carbon-coated copper grid. To assay crystallinity, the X-ray diffraction (XRD) profile was obtained on a Siemens D5000 X-ray diffractometer (scanning rate 0.05 deg/s, Cu-Kα radiation with λ= 0.154 nm). Raman spectra were both acquired using a Renishaw inVia Raman microscope equipped with a He-Cd source at 325 nm. The samples were prepared by drop-casting the dispersion onto a glass slide. Thermal analysis was performed for a cycle of 60 minutes at a constant heating rate of 10°C/min on a Mettler Toledo thermogravimetric analyser with approximately 3 mg of zinc stearate and nitrogen as the carrier gas.

Results and discussion

According to thermogravimetric analysis (Fig. 1), zinc stearate is thermally stable up to ~350°C and a significant weight loss due to the exothermic reaction of fatty acids only occurs beyond 400°C. Differential scanning calorimetry (DSC) in agreement with this trend also indicates that while the organometallic compound melts at about 128°C, the reactions continue to be largely endothermic before ~400°C. Right at the onset of decomposition, that is between 250°C and 350°C, variations in heat flow become negligible.

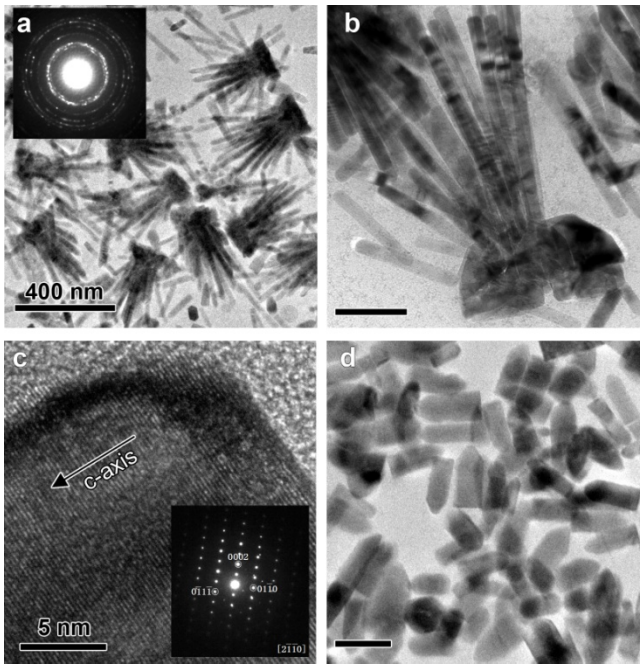

Fig 2. (a) TEM micrograph shows the abundance of bundles grown in presence of equal molar concentrations of oleylamine and oleic acid. The inset shows the selected area electron diffraction (SAED) pattern of the polycrystalline stem. (b) In absence of secondary carboxylic acids, the tectons only partially assemble. The HRTEM micrograph of (c) gives a closer view of the facing non-polar faces in the stem which is monocrystalline as evident from the SAED pattern. (d) At low concentrations of carboxylic acids, the growth is uniform and the resulting structures resemble a more extended variation of nanobullets (see Fig. 4d also). The scale bars denote 100 nm unless indicated otherwise.

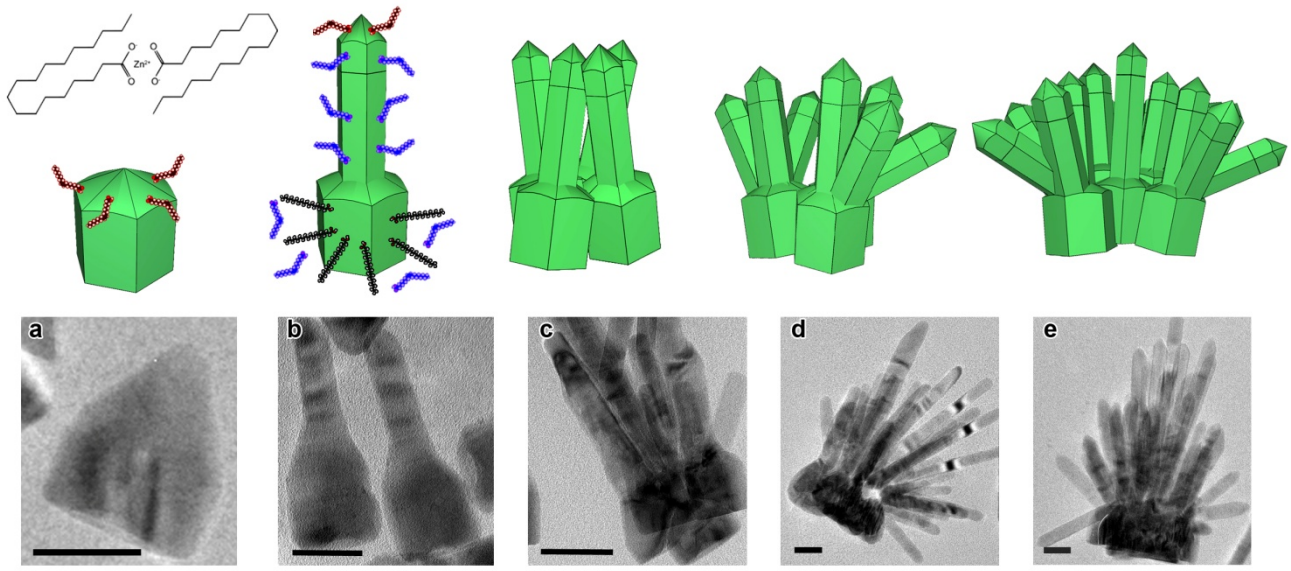

Fig. 4. The lipophilic surface chemistry of the precursor (zinc stearate) along with the mechanism of asymmetric growth and self-assembly is shown. (a) In presence of secondary carboxylic acid (here the unsaturated oleic acid shown in red), small nanobullets are initially formed. For comparison, see Fig. 5d as well. (b) The lipophilic aliphatic chains (black) inhibit the interaction of hydrophilic heads in amines (blue) with the non-polar faces in early stages, giving rise to a multi-step growth. (c) The asymmetric nanorods self-assemble into bundles and undergo recrystallisation (d). As more planar defects are formed due to diffusion at the boundaries, secondary nucleation becomes more common (e). TEM micrographs including those of both underdeveloped structures and the completely assembled bundles are taken from as-synthesised samples from the same batch. All scale bars indicate 40 nm.

Potential reactions leading to the decomposition includes formation of aerosol and condensed vapour of stearic acid followed by decarboxylation of stearate at higher temperatures and release of carbon dioxide, methane and ethylene in the subsequent stages.[25] During the stage where the rate of heat flow is nearly zero, the mediating behaviour of fatty acid chains still persists, but the temperature is high enough that with prolonged annealing, one would expect a complete pyrolysis to eventually take place and ZnO to form. The thermodynamic balance of the competing forces of decomposition (organic) and nucleation (inorganic) provides an interesting environment for studying the transition from the organically-driven polarity of lipids to that of different ZnO faces. To attest this idea, we initially studied a non-hydrous reaction under thermal equilibrium with equal molar concentrations of two of the most commonly used capping agents; an amine (oleylamine) and a carboxylic acid (oleic acid) for non-polar and polar adsorption, respectively. The resulting ZnO nanostructures were crown-like bundles of nanorods (Fig. 2) which at first glance appeared to be a form of acicular growth from a highly stable basal plane. Upon a closer investigation however, it was found that the main stem is in fact polycrystalline and consists of a large number of smaller grains. A typical X-ray diffraction profile of these bundles is given in Fig. 3.

In order to shed light on the mechanism of growth, we repeated the experiment under the same conditions, but with oleylamine alone. To our surprise, although the structures were morphologically similar to the earlier bundles, majority of them had only a pair of monocrystalline stems with clearly defined and opposing non-polar faces. Comparatively, they also showed a smaller number of nanorods branching out from their stems. Further inspection of the samples revealed that the branching structures possibly start as ZnO nanobullets (Fig. 4a) which undergo a double-step growth to produce asymmetric nanorods as those shown in Fig. 4b. These asymmetric structures later self-assemble into bundles (Fig. 4c) by aligning their highly stable basal plane[26] rather than the sharp tips and subsequently, their stem recrystallises due to boundary diffusion. Recrystallisation is likely to be accompanied by development of planar defects which is known to induce secondary nucleation on non-polar faces.[27] This scenario is in agreement with the abundance of branching in the first series of experiments where the stems are polycrystalline.

The asymmetric growth on the other hand can be explained in terms of lipophilic interactions between capping ligands and the zinc stearate prior to and after decomposition. The illustrations in Fig. 4 depict this multi-step kinetics of growth wherein the hydrophilic heads of amines (blue chains) in early stages of growth are inhibited by the hydrophobic tails of stearic acid (black chains).

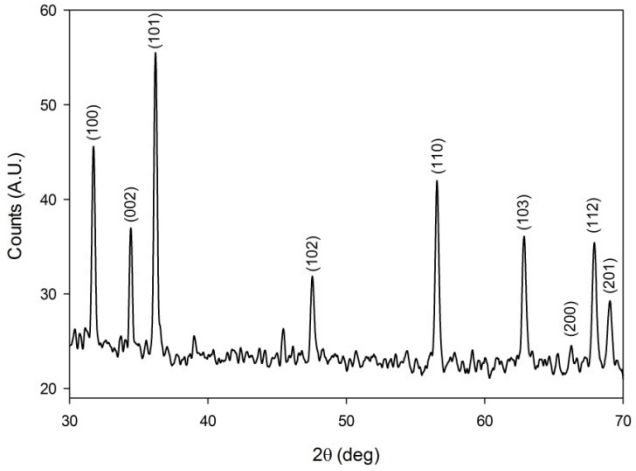

Fig. 3. X-ray diffraction profile of a typical batch of nanobundles grown in presence of oleylamine and oleic acid.

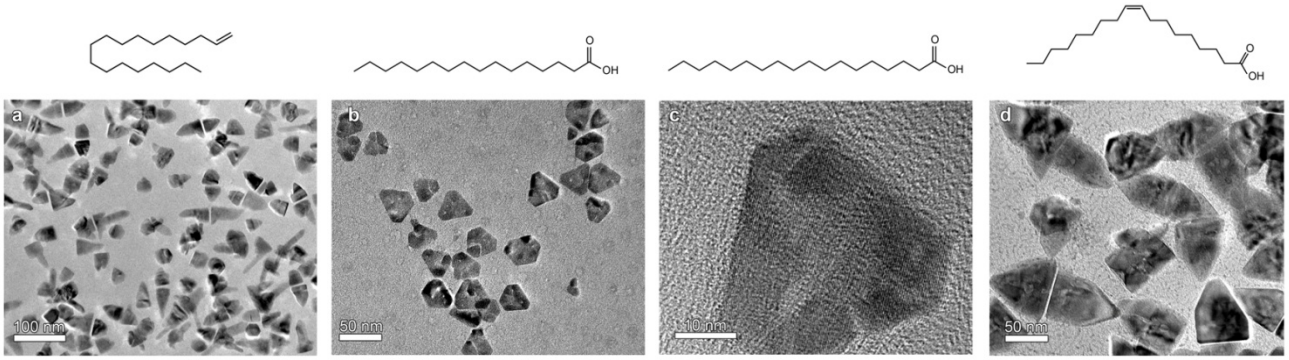

Fig. 5. The evolution of ZnO nanostructures grown using (a) only the solvent (1-octadecene) versus various carboxylic acids, including palmitic acid (b), stearic acid (c), both of which are saturated, and oleic acid (d) which is unsaturated. In the case of (b) and (c), the difference in length of lipophilic tails did not seem to have any significant effect. The growth is very rapidly terminated in the c-axis and very thin pellets with high symmetry are formed. With oleic acid although, the structures grow a base before the progression is stopped, leading to bullet-like morphologies.

It is generally understood that amines selectively attach to the non-polar facets in ZnO through forming inner sphere complexes involving carboxylates and zinc atoms.[12] These adsorbed molecules require excessive energy to be displaced and therefore hinder the growth on the $(10\bar{1}0)$ face[12,28] although in early stages of growth while stearic acid chains still cover the ZnO embryos, non-polar aliphatic tails could effectively inhibit the hydrophilic head of the amines from coming into direct contact with ZnO. As the organic ligands decompose in later stages, oleylamine eventually gets to further constrict the growth to [0001] direction and hence lead to a multi-step growth.

We noticed that the asymmetric growth behaviour was considerably more frequent in the first experiments (in presence of oleic acid) whereas with oleylamine alone, the nanobullet morphology was more dominant. Because of its chemical similarities to stearic acid (both compounds are carboxylic acid), it is plausible that oleic acid may have substituted for the decomposing ligands (to form an oleate) and contributed to the multi-step mode of growth. The idea of substitution by carboxylic acids was confirmed by replicating the experiment with other lipids (Fig. 5). In the case of stearic acid and palmitic acid, both being saturated lipids similar to the precursor's surface chemistry, the growth was rapidly terminated and two-dimensional triangular or hexagonal nanopellets were formed (thinness is due to selective adsorption to the polar face). Similar structures were synthesised in our earlier works using zinc oleate as precursor and oleic acid as capping agent.[29] In the case of zinc stearate on the other hand, oleic acid as an unsaturated lipid only terminates the growth after an initial acceleration along the c-axis. Under such circumstances, the uniform growth is very well maintained along the dipole moment creating nanobullets similar to those found in the initial experiments (Fig. 5d). This further suggests that substitution by capping molecules is dependent on the surface chemistry of the precursor and the largest constriction in growth direction (hence, pellet-like structures) takes place when matching soaps and ligands (saturated versus unsaturated) are used. The efficacy of substitution however, appears to be largely dependent on the relative concentration of ligands. In another experiment, by increasing the molar concentration of oleylamine to twice that of oleic acid, elongated nanobullets were formed (Fig. 2d). This implies that the small amount of oleic acid was not sufficient to substitute for the decomposing carboxylic acid chains on the faces, and oleylamine as expected from previous reports attached to the non-polar faces, accelerating the growth along the c-axis[28] until it was finally terminated by oleic acid. Lack of capping in the solvent (1-octadecene) generally led to formation of mostly irregular crystals with very sharp tips because of the inherently higher rate of progression in the [0001] direction. However, successful control over the morphology of similar ZnO structures at mesoscale have been achieve while suing ionic liquids as solvent.[30]

To elucidate the influence of lipids, especially the role of carboxylic acids on evolution of self-assembled bundles, we performed Raman spectroscopy for nanobullets (blue graph) as well as crown-like bundles (red graph). As demonstrated in Fig. 6, the vibrational modes of ZnO are pronounced in both samples.[31] The peak at ~574 cm^{-1} represents the first-order longitudinal optical (LO) phonon with a predominantly polar A_1 symmetry at the Γ point of BZ. The broad features from ~830 cm^{-1} to ~950 cm^{-1} can be attributed to the phonon-phonon scattering of longitudinal modes at the L and M points of BZ, while the peak at ~1078 cm^{-1} is the phonon-phonon scattering of TO and LO modes at the M-L line. Furthermore, second- and third-order A_1(LO) bands appear at ~1142 cm^{-1} and 1723 cm^{-1}, respectively.[32]

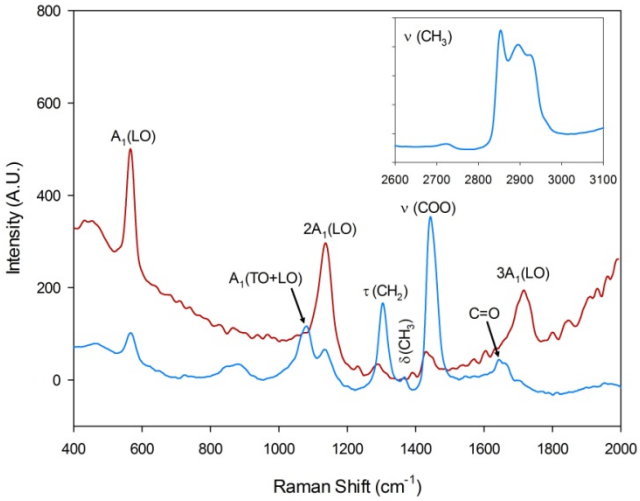

Fig. 6. The Raman spectra for the nanobullets (blue) and the bundles (red). Generally, the amount of organic constituents (derivatives of stearic acid) in the bundles is significantly smaller.

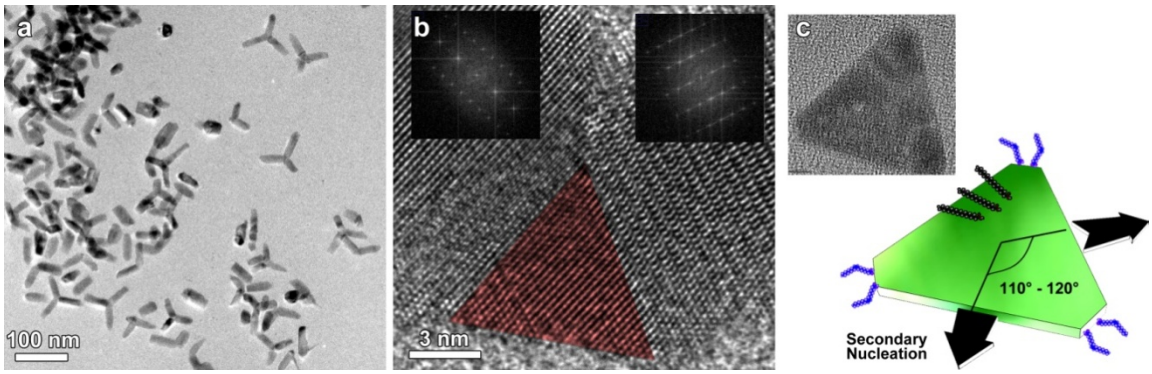

Fig. 7. Tripodal pellets (a) grown in presence of stearic acid and oleylamine start as thin triangular pellets such as those grown in presence of stearic acid alone (Fig. 5 and inset of panel c). The direction of growth outward from the stem as calculated from FFT patterns (b) indicates an angular difference of 110° to 120° which agrees well with the geometry of triangular pellets. (c) The thinness of structures can be associated with the early adsorption of stearic acid (black chains) to the polar facets while in later stages adsorption of oleylamine (blue chains) onto non-polar facets direct the secondary nculeation.

Here, we need to emphasise that the vibrational behaviour of ZnO nanostructures is highly dependent on morphology[33] as well as excitation wavelength.[34] For example, in the UV regime (e.g. 325 nm beam, also used in this study) which is close to the bandgap energy of ZnO, the stronger resonance of the polar LO modes generally dominates the resonant Raman scattering[34,35] whereas in the off-resonance visible regime (e.g. 514 nm beam), the non-polar E_2 bands, especially the high mode at ~438 cm^{-1} is the predominant feature.[36,37] The vibrational modes for the organic ligands[38] on the other hand includes the twist mode[39] of methylene (CH_2) at ~1306 cm^{-1} and the symmetric out of plane deformation (bending mode) of the methyl terminus (CH_3) at ~1370 cm^{-1} as well as its symmetric and asymmetric vibrations between 2800 cm^{-1} and 3000 cm^{-1}. For the hydrophilic head of the carboxylic acids, we have the symmetric stretching of the carboxyl (-COO) functional groups at 1444 cm^{-1} and that of carbonyl subgroups (C=O) at 1660 cm^{-1}.[40] There is no trace of vibrational modes beyond 3000 cm^{-1} where we expect to see[41] distinctive features (such as carbon double bonds) of alkene in unsaturated lipids or oleylamine. It is evident that the self-assembled bundles have only trace amounts of stearic acid adsorbates which explains their coagulation and recrystallisation. In nanobullets as well as partially assembled bundles on the contrary, the more significant presence of organic ligands obstructs van der waals attraction. Therefore, the mechanism of self-assembly and more importantly, the subsequent secondary nucleation, as the bundle undergoes recrystallisation, is directly related to the lipid-mediated growth of building blocks. Carboxylic acids and this particular case, stearic acid, appear to dictate the initial mode of growth while soon after decomposition, the effect of amines become dominant.

In order to reconfirm the proposed role of stearic acid, we performed another series of experiments with equal molar concentrations of oleylamine and stearic acid. As expected, the process of growth in the resulting structures was further inhibited by stearic acid on polar facets and initially led to the same thin triangular pellets as those seen in Fig. 5. In later stages, adsorption of oleylamine onto non-polar facets directed the secondary nucleation from the sides to create tripodal structures (see Fig. 7). The direction of growth as calculated from Fast Fourier Transform (FFT) patterns of several pellets further shows that the angular difference in growth is between 110° to 120° which is in agreement with the idea of secondary nucleation from a thin triangular pellet. A similar mechanism of growth has been previously reported for microscale tripods formed during a catalyst-free vapour-solid process using pure zinc as precursor.[42]

It is worthy of note that in contrast to the earlier experiments, the tripodal pellets are very symmetric along their c-axis which suggests that asymmetry and the following self-assembly is likely to originate from substitution of unsaturated fatty acids such as oleic acid. This variation can also be related to the surface chemistry of the precursor (here, a stearate which is similar to a saturated fatty acid).

Conclusions

We demonstrated a new approach toward engineering of iono-covalent nanomaterials using lipophilic precursors. A combination of inhibitory interactions between the surface ligands, lipids as well as hydrophilic heads in amines at optimal concentrations induce peculiar modes of growth, capable of giving rise to asymmetric nanorods. Self-assembly in these nanorods can be associated with their high surface energy and the gradual decomposition of organic ligands which bring individual building blocks in the size focus regime closer to one another. Shortly after self-assembly, the stems diffuse into one another at the boundaries upon which they recrystallise and form planar defects, followed by secondary nucleation. Moreover, decomposition of metal soaps and the process of nucleation can be mediated by matching ligands (e.g. oleates and oleic acid, stearates and stearic acid, palmitates and palmitic acids, etc). Overall, lipid-mediated growth and self-assembly is a promising step toward controlling the properties of matter at nanoscale just as how nature has intended. Future work on a larger number of lipids, especially with a focus on optimising a technique based on saturated versus unsaturated fatty acids to tune specific properties is necessary.

Acknowledgements

This study was funded by the High Impact Research Program under Project No. UM.C/625/1/HIR/079. Additional sources of funding from e-Sciencefund (13-02-03-3093), FRGS (FP003-

2011A), ERGS (ER002-2013A), HIR-MOHE (UM.C/625/1/HIR/MOHE/SC/06) and UMRG (RP007B-13AFR) are also highly appreciated. We express our gratitude to Amir Shah Sigara and Mohamad B. Aruf for analytical supports and to Prof. Lam Sai Kit for constructive discussions.

Notes and references

[a] *Low Dimensional Materials Research Centre, Department of Physics, University of Malaya, Kuala Lumpur 50603, Malaysia. Fax: +603-79674146; Tel+60 193292772; E-mail: w.s.chiu@um.edu.my*
[b] *Centre for High Impact Research, University of Malaya, Kuala Lumpur 50603, Malaysia. Fax: +60379675330; Tel: +60173470750; E-mail: yaghoubi@siswa.um.edu.my*
[c] *Faculty of Engineering, University of Nottingham Malaysia Campus, Selangor 43500, Malaysia*
[d] *Department of Materials Science and Engineering, National Tsing Hua University, Hsinchu 30013, Taiwan, R.O.C.*

1 S. Mann, *Nature*, 1993, **365**, 499.
2 H. Cölfen and S. Mann, *Angew. Chem. Int. Ed.*, 2003, **42**, 2350.
3 X. Wang, J. Zhuang, Q. Peng and Y. Li, *Nature*, 2005, **437**, 121.
4 J. Park, K. An, Y. Hwang, J.G. Park, H.J. Noh, J.Y. Kim, J.H. Park, N.M. Hwang and T. Hyeon, *Nature Mater.*, 2004, **3**, 891.
5 Z.L.Wang, *ACS Nano*, 2008, **2**, 1987.
6 Z.K. Tang, G.K. Wong, P. Yu, M. Kawasaki, A. Ohtomo, H. Koinuma and Y. Segawa, *Appl. Phys. Lett.*, 1998, **72**, 3270.
7 J.H. Lim, C.K. Kang, K.K. Kim, I.K. Park, D.K. Hwang, S.J. Park, *Adv. Mater.*, 2006, **18**, 2720.
8 Q.F. Zhou, C. Sharp, J.M. Cannata, K.K. Shung, G.H. Feng and E.S. Kim, *Appl. Phys. Lett.*, 2007, **90**, 113502.
9 J. Xu, Q. Pan, Y.A. Shun and Z. Tian, *Sensors Actuat. B-Chem*, 2000, **66**, 277.
10 N. Kumar, A. Dorfman and J.I. Hahm, *Nanotechnology*, 2006, **17**, 2875.
11 T. Nann and J. Schneider, *Chem. Phys. Lett.*, 2004, **384**, 150.
12 N.J. Nicholas, G.V. Franks and W.A. Ducker, *Langmuir*, 2012, **28**, 7189.
13 D.K.J.H. Andeen, J.H. Kim, F.F. Lange, G.K. Goh and S. Tripathy, *Adv. Funct. Mater.*, 2006, **16**, 799.
14 E.M. Wong, P.G. Hoertz, C.J. Liang, B.M. Shi, G.J. Meyer and P.C. Searson, *Langmuir*, 2001, **17**, 8362.
15 W. Peng, S. Qu, G. Cong and Z. Wang, *Cryst. Growth Des.*, 2006, **6**, 1518.
16 B. Liu and H.C. Zeng, *J. Am. Chem. Soc.*, 2003, **125**, 4430.
17 S. Baruah and J. Dutta, *Sci. Tech. Adv. Mater.*, 2009, **10**, 013001.
18 C. Pacholski, A. Kornowski and H. Weller, *Angew. Chem. Int. Ed.*, 2002, **41**, 1188.
19 X.G. Han, H.Z. He, Q. Kuang, X. Zhou, X.H. Zhang, T. Xu, Z.X. Xie and L.S. Zheng, *J. Phys. Chem. C.*, 2008, **113**, 584.
20 H. Xu, H. Wang, Y. Zhang, W. He, M. Zhu, B. Wang and H. Yan, *Ceram. Int.*, 2004, **30**, 93.
21 S.H. Choi, E.G. Kim, J. Park, K. An, N. Lee, S.C. Kim and T. Hyeon, *J. Phys. Chem. B,* 2005, **109**, 14792.
22 J. Xu, Y. Zhu, H. Huang, Z. Xie, D. Chen, and G. Shen, *Cryst. Eng. Comm.*, 2011, **13**, 2629.
23 L. Addadi and S. Weiner, *Angew. Chem. Int. Ed.*, 1992, **31**, 153.
24 K. Katagiri, R. Hamasaki, K. Ariga and J.I. Kikuchi, *J. Am. Chem. Soc.*, 2002, **124**, 7892.
25 K.A. Akinade, R.M. Campbell and D.A. Compton, *J. Mater. Sci.* 1994, **29**, 3802.
26 X.Y. Kong and Z.L. Wang, *Appl. Phys. Lett.*, 2004, **84**, 975.
27 T.L. Sounart, J. Liu, J.A. Voigt, M. Huo, E.D. Spoerke and B. McKenzie, *J. Am. Chem. Soc.*, 2007, **129**, 15786.
28 Z. Zhang, M. Lu, H. Xu and W.S. Chin, *Chem. Eur. J.*, 2007, **13**, 632.
29 W.S. Chiu, P.S. Khiew, D. Isa, M. Cloke, S. Radiman, R. Abd-Shukor, M.H. Abdullah and N.M. Huang, *Chem. Eng. J.*, 2008, **142**, 337.
30 X. Zhou, Z.X. Xie, Z.Y. Jiang, Q. Kuang, S.H. Zhang, T. Xu, R.B. Huang and L.S. Zheng, *Chem. Commun.*, 2005, **44**, 5572.
31 R. Cuscó, E. Alarcón-Lladó, J. Ibanez, L. Artús, J. Jiménez, B. Wang and M.J. Callahan, *Phys. Rev. B*, 2007, **75**, 165202.
32 K.A. Alim, V.A. Fonoberov, M. Shamsa and A.A. Balandin, *J Appl. Phys.*, 2005, **97**, 124313.
33 S.J. Chen, Y.C. Liu, Y.M. Lu, J.Y. Zhang, D.Z. Shen and X.W. Fan, *J. Cryst. Growth*, 2006, **289**, 55.
34 L. Bergman, X.B. Chen, J. Huso, J.L. Morrison and H. Hoeck, *J. Appl. Phys.*, 2005, **98**, 093507.
35 H.M. Cheng, K.F. Lin, H.C. Hsu and W.F. Hsieh, *Appl. Phys. Lett.*, 2006, **88**, 261909.
36 B. Kumar, H. Gong, S.Y. Chow, S. Tripathy and Y. Hua, *Appl. Phys. Lett.*, 2006, **89**, 071922.
37 R. Zhang, P.G. Yin, N. Wang and L. Guo, *Solid State Sci.*, 2009, **11**, 865.
38 T. Ishioka, Y. Shibata, M. Takahashi and I. Kanesaka, *Spectrochim. Acta Mol. Biomol.*, 1998, **54**, 1811.
39 W.R. Thompson and J.E. Pemberton, *Langmuir*, 1995, **11**, 1720.
40 S. Bordiga, C. Lamberti, G. Ricchiardi, L. Regli, F. Bonino, A. Damin, K. –P, Lillerud, M. Bjorgen and A. Zecchina, *Chem. Comm.* 2004, **20**, 2300.
41 C.W. Freudiger, W. Min, B.G. Saar, S. Lu, G.R. Holtom, C. He, J.C. Tsai, J.X. Kang and X.S. Xie, *Science*, 2008, **322**, 1857.
42 S. Mandal, A. Dhar and S.K. Ray, S. K. J. Appl. Phys., 2009, **105**, 033513.

